Journal of Alloys and Compounds 764 (2018) 840–844

Contents lists available at ScienceDirect

Journal of Alloys and Compounds

journal homepage: http://www.elsevier.com/locate/jalcom

Microwave dielectric properties of $Li_2W_2O_7$ ceramics improved by Al_2O_3 addition

Ching-Fang Tseng*, Hung-Chieh Hsu, Po-Hsien Chen

Department of Electronic Engineering, National United University, No. 1 Lien-Da, Kung-Ching Li, Miao-Li 36003, Taiwan

ARTICLE INFO

Article history:
Received 23 April 2018
Received in revised form
11 June 2018
Accepted 13 June 2018
Available online 14 June 2018

Keywords:
$Li_2W_2O_7$ ceramics
Al_2O_3 addition
Microwave dielectric properties
LTCC

ABSTRACT

The effect of Al_2O_3 addition on the densification, sintered behavior, phase composition and microwave dielectric properties of $Li_2W_2O_7$ ceramics prepared by conventional solid-state reaction method had been investigated. The structure, phase composition and surface morphology were studied by X-ray diffraction, EDX and scanning electron microscopy techniques, respectively. Only two phases $Li_2W_2O_7$ and Al_2O_3 were observed in all specimens. The sintering time of $Li_2W_2O_7$ ceramics with Al_2O_3 addition could be effectively reduced from 4 h to 2 h. The results showed that the doping of Al_2O_3 could promote the growth of uniform grain and improve effectively the quality factor and temperature coefficient of resonant frequency (τ_f). The $3Li_2W_2O_7$–Al_2O_3 ceramics sintered 700 °C for 2 h exhibited ε_r of 8.2, $Q \times f$ of 20,550 GHz, and τ_f of −112 ppm/°C. The good microwave dielectric properties and relatively low sintering temperature would make $3Li_2W_2O_7$–Al_2O_3 ceramics promising candidate as LTCC dielectrics for LTCC applications.

1. Introduction

For the Internet of Things and Tractile Internet (5th generation wireless communication systems) communication systems preparation, the frequencies of wireless communications are being continuously expanded from microwave to millimeter-wave [1,2]. To meet the specific requests and functions of 5th generation communication application, microwave dielectric materials with low dielectric constant ($\varepsilon_r < 10$) for fast signal transmission and reducing the cross coupling between conductors, low loss (high quality factor) for increasing frequency selectivity and desired temperature coefficient of resonant frequency (TCF, τ_f) for stability are becoming increasingly important. Meanwhile, the related microwave electronic components are strongly required to become highly integrative, high performance and low cost. Therefore, much attention has been paid to the low temperature co-fired ceramic technology (LTCC) in the past decade.

In recent years, tungstate ceramics are found potential candidates for the microwave applications due to the good microwave dielectric properties and low sintering temperature, such as Li_4WO_5, $LiMVO_6$ (M = Mo, W) and $Li_2A_2W_2O_9$ (A = Zn, Mg) [3–6]. Recently, triclinic structured $Li_2W_2O_7$ is one of Li_2O–WO_3 binary microwave dielectric systems [7]. $Li_2W_2O_7$ sintered at 640 °C for 4 h has a ε_r of 12.2, $Q \times f$ of 17,700 GHz, and TCF of −232 ppm/°C which make it to be a candidate compound for LTCC technology. However, considering the requirements for LTCC and ever-higher frequency in mobile communication application, the ε_r should be further reduced, and then TCF and $Q \times f$ value of ceramics should be improved respectively to ensure the high precision of higher-frequency telecommunicating devices.

Al_2O_3 ceramics have a low dielectric constant of 9.8, an ultrahigh $Q \times f$ of 360,000 GHz and a TCF of −60 ppm/°C. Yao et al. [8] reported that the $Q \times f$ value of $Ba_4Nd_{9.33}Ti_{18}O_{54}$ can be improve effectively by introducing Al_2O_3. In addition, it had been found that Al_2O_3 could restrict the grain growth of $CaSiO_3$ ceramics by surrounding their boundaries to further improve the density and $Q \times f$ value of $CaSiO_3$ ceramics [9]. The $Q \times f$ value of $CaSiO_3$ ceramics increased from 13,109 to 24,626 GHz by doping 1 wt% Al_2O_3. In this present, the Al_2O_3 is used to improve the microwave dielectric properties of $Li_2W_2O_7$ ceramics to satisfy demands of next generation (5G) communication system. The microstructures, sintered behaviors and microwave dielectric properties of $Li_2W_2O_7$–Al_2O_3 ceramics are investigated systematically.

2. Experimental procedure

The Li_2O, WO_3, Al_2O_3 with >99.9% high-purity oxide powders were used as starting materials to prepare via the conventional

* Corresponding author.
E-mail address: cftseng@nuu.edu.tw (C.-F. Tseng).

https://doi.org/10.1016/j.jallcom.2018.06.141
0925-8388/

solid-state method. Stoichiometric amount of the raw materials according to the composition of $3Li_2W_2O_7$–Al_2O_3 were weighted. The weighted powders were ball-milled for 12 h using agate balls with distilled water and then dried at 80 °C in an oven overnight. The dried powders were sieved using 200-mesh screen and calcined at 600 °C for 4 h in the air. The calcined powders were ground again by ball milling for 12 h, dried at 80 °C, mixed with 3 wt% of a 10% solution of PVA as a binder, and then forced through a 200-mesh sieve. After re-forced, the mixed powders pressed into pellets at the pressure of 150 MPa using a stainless die. The diameter of pellets is 11 mm and the height is about 5 mm for microwave dielectric property test. These pellets were preheated at 650 °C for 0.5 h to remove the organic binder and then sintered in the range of 660–740 °C for 2–8 h in air. The heating and the cooling rates were both set at 10 °C/min. The crystal structure of the sintered samples were indentified by X-ray diffraction method (XRD; Siemens D5000) using Cu-Kα radiation and a graphite monochromator in the 2θ range of 20–60°. The microstructure observations and analysis of as-fired surfaces of $3Li_2W_2O_7$–Al_2O_3 samples were characterized by a scanning electron microscopy (SEM; Philips XL40FEG, Eindhoven. The Netherlands) and an energy dispersive X-ray spectrometer (EDS). The densities of the ceramics were measured by the liquid Archimedes method. The dielectric properties were measured by the Hakki–Coleman dielectric resonator method, as modified and improved by Courtney [10,11] using a Network Analyzer (HP 8510). The temperature coefficient of resonant frequency (τ_f) was obtained by cavity method and calculated in the temperature range of 25–80 °C by following equation:

$$\tau f = \frac{f2 - f1}{f1(T2 - T1)} \quad (\text{ppm}/^\circ\text{C}) \tag{1}$$

where f_1 is the resonant frequency at T_1 and f_2 is the resonant frequency at T_2.

3. Results and discussions

Fig. 1 illustrates the X-ray diffraction patterns of $3Li_2W_2O_7$–Al_2O_3 ceramics sintered at 660–740 °C for 2 h. All the ceramics were identified triclinic phase with space group $P\bar{1}$ (2) (JCPDS card No. 73-0171) of $Li_2W_2O_7$ and tetragonal phase with space group $R\bar{3}c$ (167) (JCPDS card No. 85-1337) of Al_2O_3, which meant that $Li_2W_2O_7$ phase coexisted with Al_2O_3 phase. No other second phase was observed, indicating that there is no chemical reaction among $Li_2W_2O_7$ and Al_2O_3. Both the peak intensity of $Li_2W_2O_7$ and Al_2O_3 phases increased significantly with the increase of the sintering temperature. It is noted that, as measured with XRD, the peak position of $Li_2W_2O_7$ slightly shifted to higher degree introducing Al_2O_3, which indicated that the specimens incorporated with Al_2O_3 having smaller cell volume. The cell volume of pure $Li_2W_2O_7$ and $3Li_2W_2O_7$–Al_2O_3 is 272.72 and 260.775 nm^3, respectively. A decrease in unit cell volume indicated that the smaller Al^{3+} (0.535 A°) ions substitution for larger W^{6+} (0.6 A°) ions might occur [8] because of no other second phase formation.

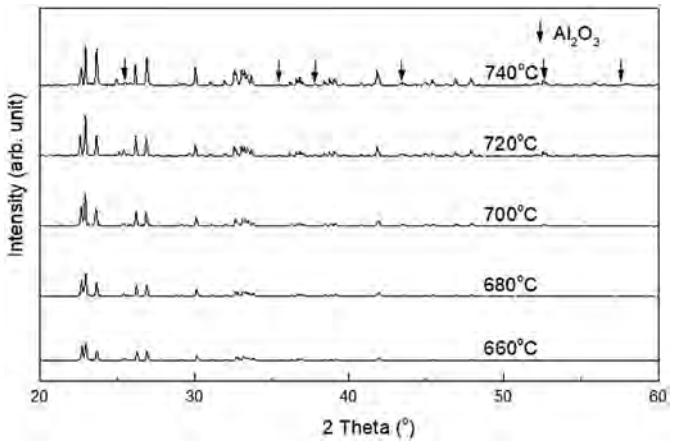

Fig. 1. XRD patterns of $3Li_2W_2O_7$–Al_2O_3 ceramics sintered at 660–740 °C for 2 h.

The SEM micrographs of the $3Li_2W_2O_7$–Al_2O_3 ceramics sintered at different conditions are illustrated in Fig. 2. It revealed that the grain size increased and porosity decreased notably with the increase in sintering temperature for 2 h. The specimen sintered at 700 °C/2 h showed significant pore elimination, densification enhancement and uniform grain distribution. However, degradation in grain uniformly started to appear at 720 °C (Fig. 3(e)), which might directly affect the microwave dielectric properties of the $3Li_2W_2O_7$–Al_2O_3 ceramics. With further increasing the firing time, comparably abnormal grain growth and the presence of pores were monitored (Fig. 3(f)-(g)) because of the over-sintering of the specimens. The local variation in growth rate of some large grains grow faster than the surrounding fine grained matrix resulted in abnormal grain growth, which could be induced by the non-uniformities in impurity content, liquid phases or porosity. No other second phase occurred in $3Li_2W_2O_7$–Al_2O_3 ceramics to control the grain growth speed by particle pinning effect [12].

Fig. 3 shows the bulk density of the $3Li_2W_2O_7$–Al_2O_3 ceramics sintered at 660–740 °C for 2–8 h. In all specimens, the densities of the specimens increased to a maximum value when the sintering temperature reached at 700 °C due to the decrease in the number of pores and the grain growth enhancement as observed in SEM. However, the densities decreased with further increasing sintering temperature and time, which allow for the variation of grain shapes in Fig. 2. It suggested that excessive sintering conditions would have no benefits of $3Li_2W_2O_7$–Al_2O_3 ceramics. In addition, the density of $Li_2W_2O_7$ decreased by introducing Al_2O_3 because a direct correlation is Al_2O_3 with a relatively lower density of 3.983 g/cm^3. The density of pure $Li_2W_2O_7$ is about 5.72 reported in Ref. [7].

Fig. 4 shows the dielectric constant of the $3Li_2W_2O_7$–Al_2O_3 ceramics sintered at 660–740 °C for 2–8 h. Generally, the dielectric constant is dominated by ionic polarizabilities of the composition, density and second phases [13]. In this paper, dielectric constant of the $3Li_2W_2O_7$–Al_2O_3 ceramics was mainly dependent on the density of ceramics. The dielectric constant of specimens was approximately proportional to the bulk density of specimens. It was known that higher density would lead to higher dielectric constant due to the less pore ($\varepsilon_r = 1$). When sintered at 700 °C for 2 h, $3Li_2W_2O_7$–Al_2O_3 ceramics achieved a high dielectric constant of 8.2. Moreover, the dielectric constant decreased with increasing sintering time.

Fig. 5 presents the $Q \times f$ value of $3Li_2W_2O_7$–Al_2O_3 ceramics sintered at different conditions. The microwave dielectric loss includes not only intrinsic loss caused by absorption of phonon oscillation but also extrinsic losses caused by impurity, substitution, pores, size and shapes of grains, second phase, etc [13,14]. The $Q \times f$ value of $3Li_2W_2O_7$–Al_2O_3 ceramics showed a similar trend by changing density. It indicated that the $Q \times f$ value was closely related to its corresponding density in this work. The $Q \times f$ value of samples sintered at 660 and 680 °C were relatively low owing to the low densities and porous microstructures. By increasing the sintering temperature, $Q \times f$ value reached to the maximum value at 700 °C and decreased thereafter. The highest $Q \times f$ value of 20,550 GHz was obtained for $3Li_2W_2O_7$–Al_2O_3 ceramics sintered at 700 °C/2 h. The $Q \times f$ values decreased with further long-time firing. For high-temperature and long-time sintering, the degradation of

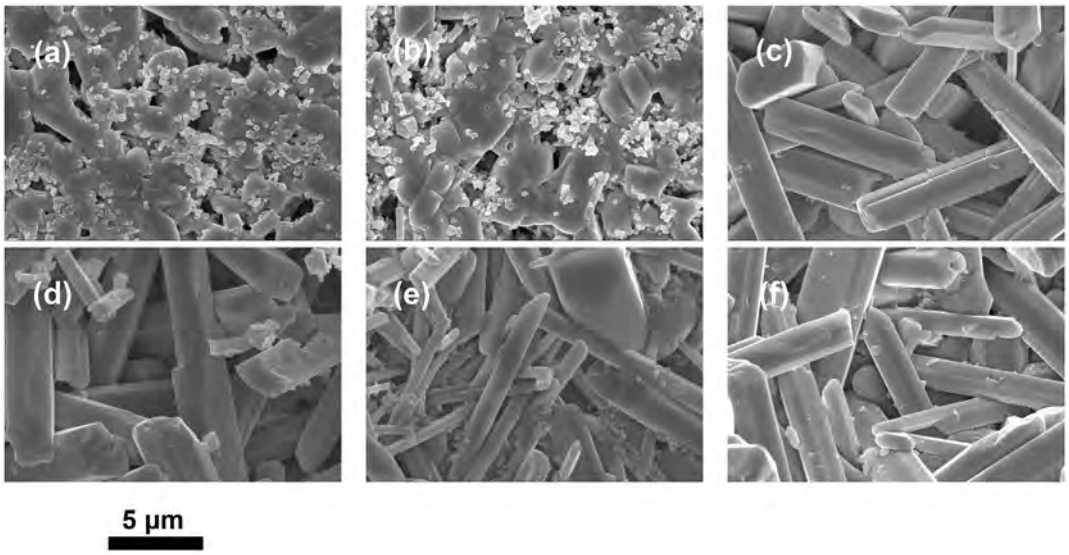

Fig. 2. SEM micrographs of $3Li_2W_2O_7$–Al_2O_3 ceramics sintered at (a)–(e) sintered at 660–740 °C for 2 h and (f)–(g) 700 °C for 4 h and 6 h, respectively.

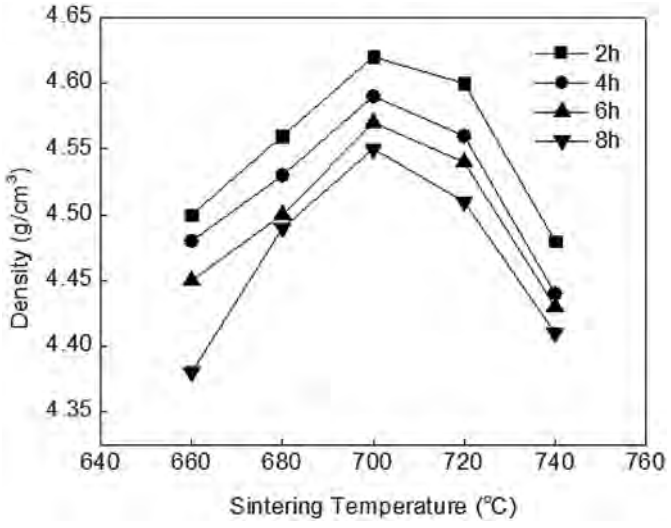

Fig. 3. Bulk densities of $3Li_2W_2O_7$–Al_2O_3 ceramics fired at various sintering conditions.

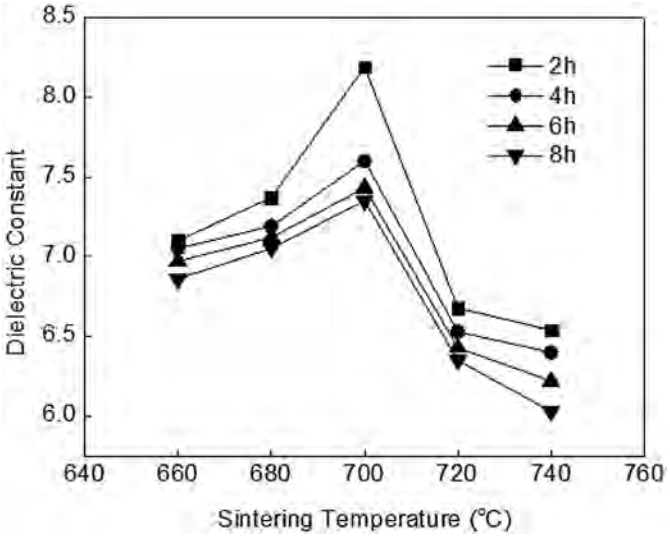

Fig. 4. The variations of dielectric constant of $3Li_2W_2O_7$–Al_2O_3 ceramics fired at various sintering conditions.

$Q \times f$ values was attributed to abnormal grain growth that might be resulted in the presence of pores as seen in Fig. 2. Notice that the $Q \times f$ value of $3Li_2W_2O_7$–Al_2O_3 ceramics was higher than pure $Li_2W_2O_7$ (17,700 GHz). The improvement of the $Q \times f$ value of $3Li_2W_2O_7$–Al_2O_3 ceramics was explained by adding Al_2O_3 with high $Q \times f$ value and the increase in the grain size.

The theoretical permittivity of $3Li_2W_2O_7$–Al_2O_3 composites, sintered at 700 °C for 2 h, can be calculated by different mixing formulas. The well-known general empirical equations for predicting dielectric constant of a compound are as following [15–22]:

Series mixing model:

$$\frac{1}{\varepsilon_{mix}} = \frac{(1-x)}{\varepsilon_{r1}} + \frac{x}{\varepsilon_{r2}} \quad (2)$$

Parallel mixing model:

$$\varepsilon_{mix} = (1-x)\varepsilon_{r1} + x\varepsilon_{r2} \quad (3)$$

Brick-Wall:

$$\varepsilon_{mix} = \varepsilon_{r2}\left(1 - \frac{1-x}{1-n}\right) + \left(\frac{1-x}{1-n}\right)\frac{\varepsilon_{r1}\varepsilon_{r2}}{(1-n)\varepsilon_{r2} + n\varepsilon_{r1i}}, n = \frac{x}{3} \quad (4)$$

Lichtenecker empirical logarithmic model:

$$\ln \varepsilon_{mix} = (1-x)\ln \varepsilon_{r1} + x \ln \varepsilon_{r2} \quad (5)$$

EMT:

$$\varepsilon_{mix} = \varepsilon_{r2}\left[1 + \frac{x(\varepsilon_{r1} - \varepsilon_{r2})}{\varepsilon_{r2} + nx(\varepsilon_{r1} - \varepsilon_{r2})}\right] \text{ (for n } = 0.165) \quad (6)$$

Jayasundere-Smith:

$$\varepsilon_{mix} = \frac{\varepsilon_{r2}x + \varepsilon_{r1}(1-x)[3\varepsilon_{r2}/(\varepsilon_{r1}+2\varepsilon_{r2})][1+3(1-x)(\varepsilon_{r1}-\varepsilon_{r2})/(\varepsilon_{r1}+2\varepsilon_{r2})]}{x+(1-x)(3\varepsilon_{r2})/(\varepsilon_{r1}+2\varepsilon_{r2})[1+3(1-x)(\varepsilon_{r1}-\varepsilon_{r2})/(\varepsilon_{r1}+2\varepsilon_{r2})]} \quad (7)$$

Poon-Shin:

$$\varepsilon_{mix} = \varepsilon_{r2}\left[1+\frac{(1-x)((\varepsilon_{r1}/\varepsilon_{r2})-1)}{(1-x)+(x/3)[(\varepsilon_{r1}/\varepsilon_{r2})x+(1-x)+2]}\right] \quad (8)$$

where ε_{mix}, ε_{r1}, and ε_{r2} are dielectric constants of a $3Li_2W_2O_7$–Al_2O_3 composite, $Li_2W_2O_7$, and Al_2O_3, respectively. (1−x) and x are the volume fraction of each phase with respect to ε_{r1} and ε_{r2}. The dielectric constant of $3Li_2W_2O_7$–Al_2O_3 ceramics predicted from above mixture rules are shown in Table 1. From this Table it was evident that out of all calculated results, the measured permittivity of composites didn't agree well with the calculated values. The deviation of permittivity from the predicted mixing rules may be due to the porosity. The influence of porosity on dielectric constant can be diminished by applying below correction equations, shown in Eq. (9)–(11) [23,24]:

$$\varepsilon_{corr} = \varepsilon_{mix} + \frac{3P\varepsilon_{mix}(1-\varepsilon_{mix})}{1+2\varepsilon_{mix}-P(1-\varepsilon_{mix})} \quad (9)$$

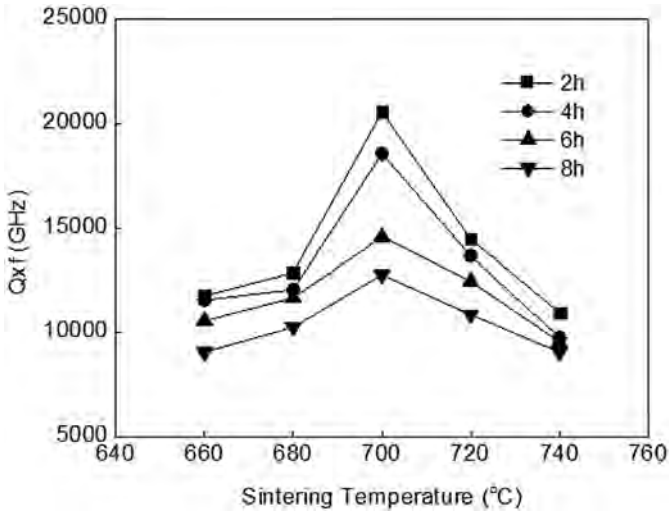

Fig. 5. The variations of $Q \times f$ value of $3Li_2W_2O_7$–Al_2O_3 ceramics fired at various sintering conditions.

Table 1
The measured, calculated and corrected dielectric constant of $3Li_2W_2O_7$–Al_2O_3 ceramics.

Measured ε_r	Calculated ε_r form Eqs. (2)–(8)	Calculated ε_r after correcting porosity by		
		Eq. (9)	Eq. (10)	Eq. (11)
8.2	11.496	8.720	8.478	8.843
	11.600	8.800	8.551	8.923
	11.564	8.771	8.526	8.895
	11.550	8.761	8.516	8.885
	11.582	8.740	8.539	8.909
	11.441	8.681	8.440	8.801
	11.591	8.790	8.545	8.916

$$\varepsilon_{corr} = \varepsilon_{mix} + \frac{3P\varepsilon_{mix}(1-\varepsilon_{mix})}{1+2\varepsilon_{mix}} \quad (10)$$

$$\varepsilon_{corr} = \frac{\varepsilon_{mix}}{1+1.5P} \quad (11)$$

where ε_{corr}, ε_{mix}, and P are corrected permittivity and calculated permittivity, and porosity of $3Li_2W_2O_7$–Al_2O_3 ceramics, respectively. The calculated ε_r after correcting porosity by Eq. (9)–(11) are also shown in Table 1. The corrected dielectric constants were most closed to the measured data.

The $Q \times f$ value are affected by densification. The tanδ suggests that the porosity dependence can be obtain from the following equations [23]:

$$\tan\delta = \tan\delta_0 + AP^n \quad (12)$$

where $\tan\delta_0 = 5 \times 10^{-4}$ is the minimum loss of $3Li_2W_2O_7$–Al_2O_3 ceramics and $AP^n (A = 1.515 \times 10^{-4}, n = 1.36)$ is the loss contribution from the pore in the $3Li_2W_2O_7$–Al_2O_3 ceramics. The porosity of $3Li_2W_2O_7$–Al_2O_3 ceramics is 0.2. Another model is []

$$\tan\delta = (1-P)\tan\delta_0 + PA\left(\frac{P}{1-P}\right)^{1/3} \quad (13)$$

where $\tan\delta_0 = 5 \times 10^{-4}$ and $A = 2.219 \times 10^{-4}$, respectively. Table 2 presents the corrected $Q \times f$ values of $3Li_2W_2O_7$–Al_2O_3 ceramics. Eqs. (12) and (13) can give a good fit to the measured data. From Tables 1 and 2 results it is concluded that the dielectric constant and $Q \times f$ value of $3Li_2W_2O_7$–Al_2O_3 ceramics are strongly dominated by the presence of porosity.

Fig. 6 illustrates the temperature coefficient of resonant frequency (TCF, τ_f) of the $3Li_2W_2O_7$–Al_2O_3 ceramics sintered at 660–740 °C for 2–8 h. The τ_f values are governed by additives, the existence of second phases, and the composition. The τ_f values were not sensitive to different sintering conditions because of no alternative composition. Hence, the τ_f values were almost in the range of −120 ~ −130 ppm/°C in this experiment. The Al_2O_3 phase possesses relatively high τ_f value (−60 ppm/°C), which lead to an increase in the τ_f values of the $3Li_2W_2O_7$–Al_2O_3 ceramics.

4. Conclusion

The microstructure, sintering behavior and microwave dielectric properties of $3Li_2W_2O_7$–Al_2O_3 ceramics prepared via conventional solid-state reaction method had been investigated in this present. No other second phases were detected by XRD besides $Li_2W_2O_7$ and Al_2O_3. To introduce Al_2O_3 into $Li_2W_2O_7$ ceramics can improve the $Q \times f$ and τ_f values of $Li_2W_2O_7$ ceramics because of Al_2O_3 with

Table 2
The measured and corrected $Q \times f$ value of $3Li_2W_2O_7$–Al_2O_3 ceramics.

Measure $Q \times f$ (GHz)	Corrected $Q \times f$ by	
	Eq. (12)	Eq. (13)
20,550	23,200	28,050

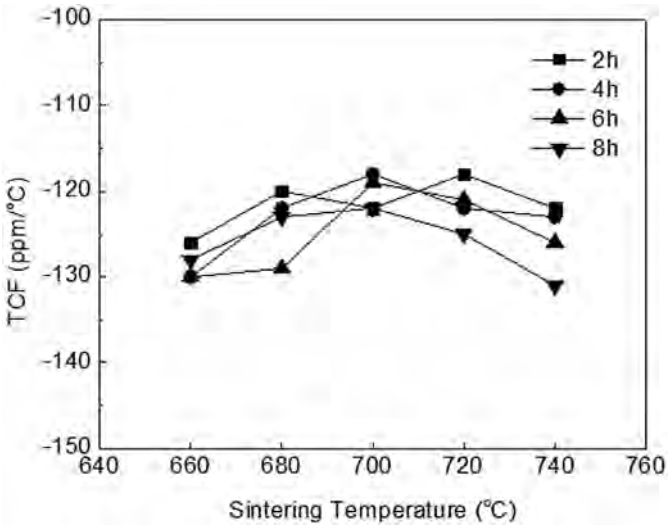

Fig. 6. The variations of τ_f of $3Li_2W_2O_7$–Al_2O_3 ceramics fired at various sintering conditions.

favourable conditions of them. The grain growth, densification of $3Li_2W_2O_7$–Al_2O_3 ceramics, which affected the microwave dielectric properties, were changed with various sintering conditions. Higher density indicated lower porosity, therefore the relationship between microwave dielectric properties process was interpreted through the variation of microstructures. The ε_r and $Q \times f$ values decreased due to deterioration of density, abnormal grain growth and the presence of pores as the specimens were at over-sintering. The optimal microwave dielectric properties of $\varepsilon_r = 8.2$, $Q \times f = 20{,}550$ GHz, and $\tau_f = -122$ ppm/°C were obtained for $3Li_2W_2O_7$–Al_2O_3 ceramics sintered at 700 °C/2 h. The results suggested it a promising ceramic for LTCC application as substrate in microwave integrated circuit for 5G communication systems preparation.

Acknowledgments

This work was sponsored by the National Science Council of the Republic of China under grant MOST 106-2221-E-239 -029.

References

[1] A. Osseiran, F. Boccardi, V. Braun, K. Kusume, P. Marsch, M. Maternia, O. Queseth, M. Schellmann, H. Schotten, H. Taoka, H. Tullberg, M.A. Uusitalo, B. Timus, M. Fallgren, Scenarios for 5G mobile and wireless communications: the vision of the METIS project, IEEE Commun. Mag. 52 (2014) 26–35.
[2] M.T. Sebastian, R. Ubic, H. Jantunen, Microwave Materials and Applications, John Wiley & Sons, 2017.
[3] J. Li, L. Fang, H. Luo, J. Khaliq, Y. Tang, C.C. Li, Li_4WO_5: a temperature stable low-firing microwave dielectric ceramic with rock salt structure, J. Eur. Ceram. Soc. 36 (2015) 243–246.
[4] H.H. Guo, L. Fang, X.W. Jiang, F.Q. Lu, C.C. Li, $Li2_Zn_2W_2O_9$: a novel low temperature sintering microwave dielectric ceramic with corundum structure, Ceram. Int. 42 (2016) 5553–5557.
[5] H.H. Guo, L. Fang, X.W. Jiang, J. Li, F.Q. Lu, C.C. Li, A novel low-firing and low loss microwave dielectric ceramic $Li_2Mg_2W_2O_9$ with corundum structure, J. Am. Ceram. Soc. 98 (2016) 3863–3868.
[6] H. Xiang, C. Li, Y. Tang, L. Fang, Two novel ultralow temperature firing microwave dielectric ceramics LiMVO6 (M = Mo, W) and their chemical compatibility with metal electrodes, J. Eur. Ceram. Soc. 37 (2017) 3959–3963.
[7] J. Chen, C. Li, D. Wang, H. Xiang, L. Fang, Preparation, Crystal structure, and dielectric characterization of $Li_2W_2O_7$ ceramic at RF and microwave frequency range, J. Adv. Dielectr. 7 (2017), 1720001-1–1720001-5.
[8] X. Yao, H. Lin, X. Zhao, W. Chen, L. Luo, Effect of Al_2O_3 addition on the microstructure and microwave dielectric properties of $Ba_4Nd_{9.33}Ti_{18}O_{54}$ ceramics, Ceram. Int. 38 (2012) 6723–6728.
[9] H.P. Wang, J.M. Chen, W.Y. Tang, S.Q. Feng, H.P. Ma, G.H. Jia, S.Q. Xu, Effects of Al_2O_3 addition on the sintering behavior and microwave dielectric properties of $CaSiO_3$ ceramics, J. Eur. Ceram. Soc. 32 (2012) 541–545.
[10] B.W. Hakki, P.D. Coleman, A dielectric resonator method of measuring inductive capacities in the millimeter range, IEEE Trans. Microw. Theor. Tech. 8 (1960) 402–410.
[11] W.E. Courtney, Analysis and evaluation of a method of measuring the complex permittivity and permeability microwave insulators, IEEE Trans. Microw. Theor. Tech. 18 (1970) 476–485.
[12] H. Wang, H. Lin, W. Li, J. Shi, Effect of La doping on microwave dielectric properties of translucent polycrystalline alumina ceramic, Ceram. Int. 39 (2013) 4097–4911.
[13] S. George, M.T. Sebastian, Synthesis and microwave dielectric properties of novel temperature stable high Q, $Li_2ATi_3O_8$ (A = Mg, Zn) ceramics, J. Am. Ceram. Soc. 93 (2010) 2164–2166.
[14] H.F. Zhou, X.B. Liu, X.L. Chen, L. Fang, Y.L. Wang, $ZnLi_{2/3}Ti_{4/3}O_4$: a new low loss spinel microwave dielectric ceramic, J. Eur. Ceram. Soc. 32 (2012) 261–265.
[15] D. Borrow, T. Petroff, R. Tandon, M. Sayer, Characterization of thick lead zirconate titanate film fabricated using a new sol gel based process, J. Appl. Phys. 81 (876) (1997) 1–6.
[16] P. Sarah, S. Suryanarayana, Dielectric properties of piezoelectric 3–0 composites of lithium ferrite/barium titanate, Bull. Mater. Sci. 26 (2003) 745–747.
[17] I. Rychetsky, J. Petzelt, Dielectric spectra of grainy high-permittivity materials, Ferroelectrics 303 (2004) 137–140.
[18] Z. Hashin, S. Shtrikman, A variational approach to the theory of the effective magnetic permeability of multiphase materials, J. Appl. Phy. 33 (1962) 3125–3131.
[19] H.H.B. Rocha, F.N.A. Freire, M.R.P. Santons, J.M. Sasaki, T. Cordaro, A.S.B. Sombra, Radio-frequency (RF) studies of the magneto-dielectric composites: $Cr_{0.75}Fe_{1.25}O_3$ (CRFO)–$Fe_{0.5}Cu_{0.75}Ti_{0.75}O_3$ (FCTO), Physica B 403 (2008) 2902–2909.
[20] Y.M. Poon, F.G. Shin, A simple explicit formula for the effective dielectric constant of binary 0-3 composites, J. Mater. Sci. 39 (2004) 1277–1281.
[21] N. Jayasundere, B.V. Smith, Dielectric constant for binary piezoelectric 0–3 composites, J. Appl. Phy. 73 (1993) 2462–2466.
[22] Y. Rao, J. Qu, T. Marinis, C.P. Wong, A precise numerical prediction of effective dielectric constant for polymer ceramic composites based on effective medium theory, IEEE Trans. Compon. Packag. Technol. 23 (2000) 680–683.
[23] W. Luo, J. Guo, G. Randall, M. Lanagan, Effect of porosity and microstructure on the microwave dielectric properties of rutile, Mater. Lett. 200 (2017) 101–104.
[24] A.J. Bosman, E.E. Havinga, Temperature dependence of dielectric constants of cubic ionic compounds, Phys. Rev. 129 (1963) 1593–1600.